

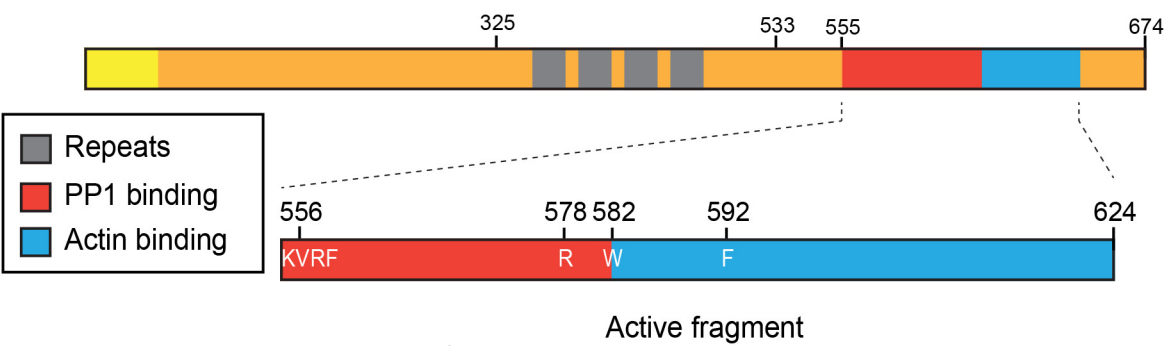


Figures and figure supplements

PPP1R15A-mediated dephosphorylation of eIF2 α is unaffected by Sephin1 or Guanabenz

Ana Crespillo-Casado et al

A Human PPP1R15A



B Active fragment

R15A_Human	555			*																																																																																																																																																																																																																																																																																																																																																																																																																																																																																																																																																																																																																																																																																																																																																																																																																																																																																																																																																																																																																																																																																																																																																																																																																																																																																																																																																																																																																																																																																																																																																																																																																																																																																																											</
-------------------	------------	--	--	---	--	--	--	--	--	--	--	--	--	--	--	--	--	--	--	--	--	--	--	--	--	--	--	--	--	--	--	--	--	--	--	--	--	--	--	--	--	--	--	--	--	--	--	--	--	--	--	--	--	--	--	--	--	--	--	--	--	--	--	--	--	--	--	--	--	--	--	--	--	--	--	--	--	--	--	--	--	--	--	--	--	--	--	--	--	--	--	--	--	--	--	--	--	--	--	--	--	--	--	--	--	--	--	--	--	--	--	--	--	--	--	--	--	--	--	--	--	--	--	--	--	--	--	--	--	--	--	--	--	--	--	--	--	--	--	--	--	--	--	--	--	--	--	--	--	--	--	--	--	--	--	--	--	--	--	--	--	--	--	--	--	--	--	--	--	--	--	--	--	--	--	--	--	--	--	--	--	--	--	--	--	--	--	--	--	--	--	--	--	--	--	--	--	--	--	--	--	--	--	--	--	--	--	--	--	--	--	--	--	--	--	--	--	--	--	--	--	--	--	--	--	--	--	--	--	--	--	--	--	--	--	--	--	--	--	--	--	--	--	--	--	--	--	--	--	--	--	--	--	--	--	--	--	--	--	--	--	--	--	--	--	--	--	--	--	--	--	--	--	--	--	--	--	--	--	--	--	--	--	--	--	--	--	--	--	--	--	--	--	--	--	--	--	--	--	--	--	--	--	--	--	--	--	--	--	--	--	--	--	--	--	--	--	--	--	--	--	--	--	--	--	--	--	--	--	--	--	--	--	--	--	--	--	--	--	--	--	--	--	--	--	--	--	--	--	--	--	--	--	--	--	--	--	--	--	--	--	--	--	--	--	--	--	--	--	--	--	--	--	--	--	--	--	--	--	--	--	--	--	--	--	--	--	--	--	--	--	--	--	--	--	--	--	--	--	--	--	--	--	--	--	--	--	--	--	--	--	--	--	--	--	--	--	--	--	--	--	--	--	--	--	--	--	--	--	--	--	--	--	--	--	--	--	--	--	--	--	--	--	--	--	--	--	--	--	--	--	--	--	--	--	--	--	--	--	--	--	--	--	--	--	--	--	--	--	--	--	--	--	--	--	--	--	--	--	--	--	--	--	--	--	--	--	--	--	--	--	--	--	--	--	--	--	--	--	--	--	--	--	--	--	--	--	--	--	--	--	--	--	--	--	--	--	--	--	--	--	--	--	--	--	--	--	--	--	--	--	--	--	--	--	--	--	--	--	--	--	--	--	--	--	--	--	--	--	--	--	--	--	--	--	--	--	--	--	--	--	--	--	--	--	--	--	--	--	--	--	--	--	--	--	--	--	--	--	--	--	--	--	--	--	--	--	--	--	--	--	--	--	--	--	--	--	--	--	--	--	--	--	--	--	--	--	--	--	--	--	--	--	--	--	--	--	--	--	--	--	--	--	--	--	--	--	--	--	--	--	--	--	--	--	--	--	--	--	--	--	--	--	--	--	--	--	--	--	--	--	--	--	--	--	--	--	--	--	--	--	--	--	--	--	--	--	--	--	--	--	--	--	--	--	--	--	--	--	--	--	--	--	--	--	--	--	--	--	--	--	--	--	--	--	--	--	--	--	--	--	--	--	--	--	--	--	--	--	--	--	--	--	--	--	--	--	--	--	--	--	--	--	--	--	--	--	--	--	--	--	--	--	--	--	--	--	--	--	--	--	--	--	--	--	--	--	--	--	--	--	--	--	--	--	--	--	--	--	--	--	--	--	--	--	--	--	--	--	--	--	--	--	--	--	--	--	--	--	--	--	--	--	--	--	--	--	--	--	--	--	--	--	--	--	--	--	--	--	--	--	--	--	--	--	--	--	--	--	--	--	--	--	--	--	--	--	--	--	--	--	--	--	--	--	--	--	--	--	--	--	--	--	--	--	--	--	--	--	--	--	--	--	--	--	--	--	--	--	--	--	--	--	--	--	--	--	--	--	--	--	--	--	--	--	--	--	--	--	--	--	--	--	--	--	--	--	--	--	--	--	--	--	--	--	--	--	--	--	--	--	--	--	--	--	--	--	--	--	--	--	--	--	--	--	--	--	--	--	--	--	--	--	--	--	--	--	--	--	--	--	--	--	--	--	--	--	--	--	--	--	--	--	--	--	--	--	--	--	--	--	--	--	--	--	--	--	--	--	--	--	--	--	--	--	--	--	--	--	--	--	--	--	--	--	--	--	--	--	--	--	--	--	--	--	--	--	--	--	--	--	--	--	--	--	--	--	--	--	--	--	--	--	--	--	--	--	--	--	--	--	--	--	--	--	--	--	--	--	--	--	--	--	--	--	--	--	--	--	--	--	--	--	--	--	--	--	--	--	--	--	--	--	--	--	--	--	--	--	--	--	--	--	--	--	--	--	--	--	--	--	--	--	--	--	--	--	--	--	--	--	--	--	--	--	--	--	--	--	--	--	--	--	--	--	--	--	--	--	--	--	--	--	--	--	--	--	--	--	--	--	--	--	--	--	--	--	--	--	--	--	--	--	--	--	--	--	--	--	--	--	--	--	--	--	--	--	--	--	--	--	--	--	--	--	--	--	--	--	--	--	--	--	--	--	--	--	--	--	--	--	--	--	--	--	--	--	--	--	--	--	--	--	--	--	--	--	--	--	--	--	--	--	--	--	--	--	--	--	--	--	--	--	--	--	--	--	--	--	--	--	--	--	--	--	--	--	--	--	--	--	--	--	--	--	--	--	--	--	--	--	--	--	--	--	--	--	--	--	--	--	--	--	--	--	--	--	--	--	--	--	--	--	--	--	--	--	--	--	--	--	--	--	--	--	--	--	--	--	--	--	--	--	--	--	--	--	--	--	--	--	--	--	--	--	--	--	--	--	--	--	--	--	--	--	--	--	--	--	--	--	--	--	--	--	--	--	--	--	--	--	--	--	--	--	--	--	--	--	--	--	--	--	--	--	--	--	--	--	--	--	--	--	--	--	--	--	--	--	--	--	--	--	--	--	--	--	--	--	--	--	--	--	--	--	--	--	--	--	--	--	--	--	--	--	--	--	--	--	--	--	--	--	--	--	--	--	--	--	--	--	--	--	--	--	--	--	--	--	--	--	--	--	--	--	--	--	--	--	--	--	--	--	--	--	--	--	--	--	--	--	--	--	--	--	--	--	--	--	--	--	--	--	--	--	--	--	--	--	--	--	--	--	--	--	--	--	--	--	--	--	--	--	--	--	--	--	--	--	--	--	--	--	--	--	--	--	--	--	--	--	--	--	--	--	--	--	--	--	--	--	--	--	--	--	--	--	--	--	--	--	--	--	--	--	--	--	--	--	--	--	--	--	--	--	--	--	--	--	--	--	--	--	--	--	--	--	--	--	--	--	--	--	--	--	--	--	--	--	--	--	--	--	--	--	--	--	--	--	--	--	--	--	--	--	--	--	--	--	--	--	--	--	--	--	--	--	--	--	--	--	--	--	--	--	--	--	--	--	--	--	--	--	--	--	--	--	--	--	--	--	--	--	--	--	--	--	--	--	--	--	--	--	--	--	--	--	--	--	--	--	--	--	--	--	--	--	--	--	--	--	--	--	--	--	--	--	--	--	--	--	--	--	--	--	--	--	--	--	--	--	--	--	--	--	--	--	--	--	--	--	--	--	--	--	--	--	--	--	--	--	--	--	--	--	--	--	--	--	--	--	--	--	--	--	--	--	--	--	--	--	--	--	--	--	--	--	--	--	--	--	--	--	--	--	--	----

C

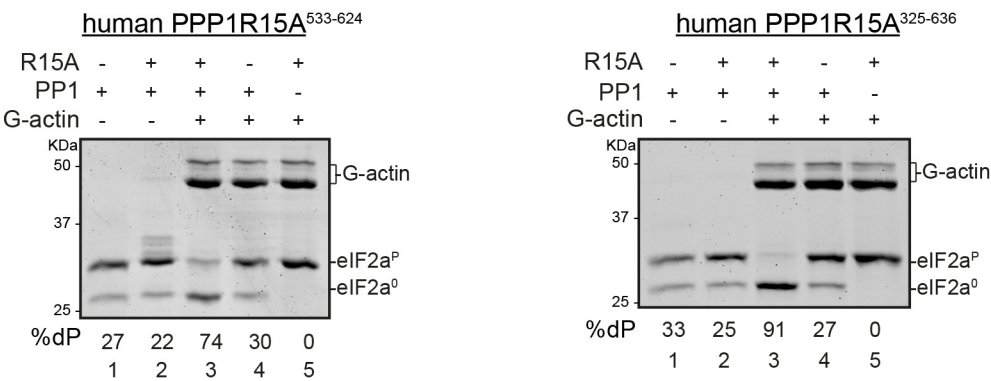


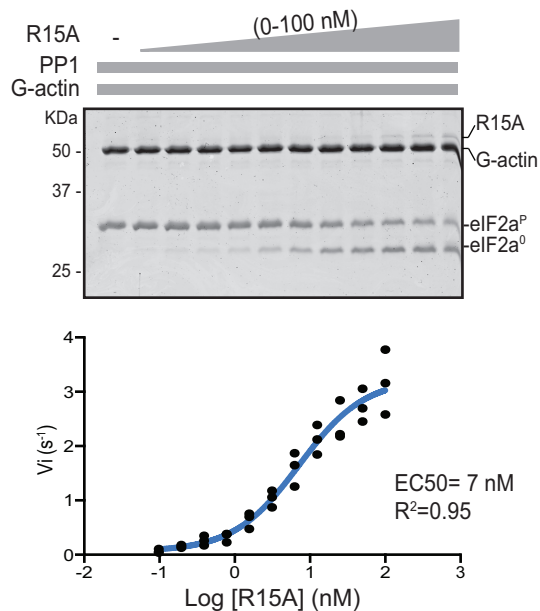
Figure 1. A tripartite assay for human PPP1R15A-dependent eIF2 α -P dephosphorylation. **(A)** Cartoon representation of human PPP1R15A (GADD34). The minimal C-terminal peptide required for eIF2 α -P dephosphorylation is outlined ('active fragment') and key residues in the PP1 and G-actin binding regions are annotated. **(B)** Alignment of C-terminal active fragments of mammalian PPP1R15A and PPP1R15B (CREP) using ClustalX. Grey highlighted residues represent conserved or highly similar residues. Red asterisks highlight key residues that are analysed in further detail. **(C)** Image of Coomassie-stained PhosTag-SDS-PAGE on which phosphorylated (eIF2 α^P) and non-phosphorylated (eIF2 α^0) forms of eIF2 α from 20 min dephosphorylation reactions were resolved. The composition of the reaction, PPP1R15A⁵³³⁻⁶²⁴ [80 nM], PPP1R15A³²⁵⁻⁶³⁶ [400 nM], PP1c [12.5 nM] and G-actin [750 nM] are noted above and the fraction of dephosphorylated eIF2 α is noted underneath each lane (%dP). The migration of molecular weight markers and G-actin are noted (the signal from the PPP1R15A and PP1c is undetectable on these gels).

DOI: [10.7554/eLife.26109.003](https://doi.org/10.7554/eLife.26109.003)

A Human PPP1R15A



B



C

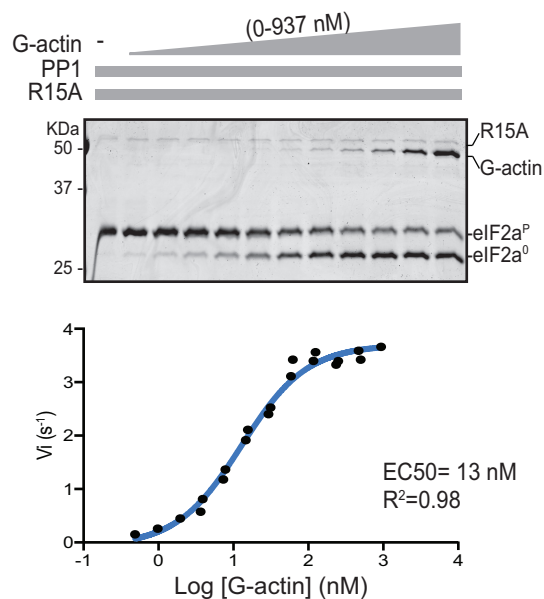


Figure 2. eIF2 α -P dephosphorylation kinetics as a function of human PPP1R15A⁵³³⁻⁶²⁴ and G-actin concentration. (A) Schema of the human PPP1R15A⁵³³⁻⁶²⁴ construct used. The C-terminal Maltose Binding Protein (MBP) component, which stabilizes the fusion protein, is noted. (B) Upper Figure 2 continued on next page

Figure 2 continued

panel. Coomassie-stained PhosTag-SDS-PAGE tracking the dephosphorylation of $eIF2\alpha^P$ to $eIF2\alpha^0$ in 20 min dephosphorylation reactions constituted with $eIF2\alpha^P$ [2 μ M], PP1 [0.625 nM], G-actin [1.5 μ M] and an escalating concentration of PPP1R15A⁵³³⁻⁶²⁴. Shown is a representative of three independent experiments performed. **Lower panel:** Semi-log₁₀ plot of the initial velocity of $eIF2\alpha^P$ dephosphorylation as a function of PPP1R15A⁵³³⁻⁶²⁴ concentration derived from three repeats (one shown above). The EC₅₀ for PPP1R15A⁵³³⁻⁶²⁴ was calculated using the agonist fitting function on GraphPad Prism V7. **(C) Upper panel.** As in 'B' but dephosphorylation of $eIF2\alpha^P$ to $eIF2\alpha^0$ was carried out in the presence of a fixed concentration of PPP1R15A⁵³³⁻⁶²⁴ [50 nM] and an escalating concentration of G-actin. Shown is a representative of two independent experiments performed. **Lower panel:** Semi-log₁₀ plot of initial velocity as a function of G-actin concentration derived from two repeats (one shown above).

DOI: [10.7554/eLife.26109.004](https://doi.org/10.7554/eLife.26109.004)

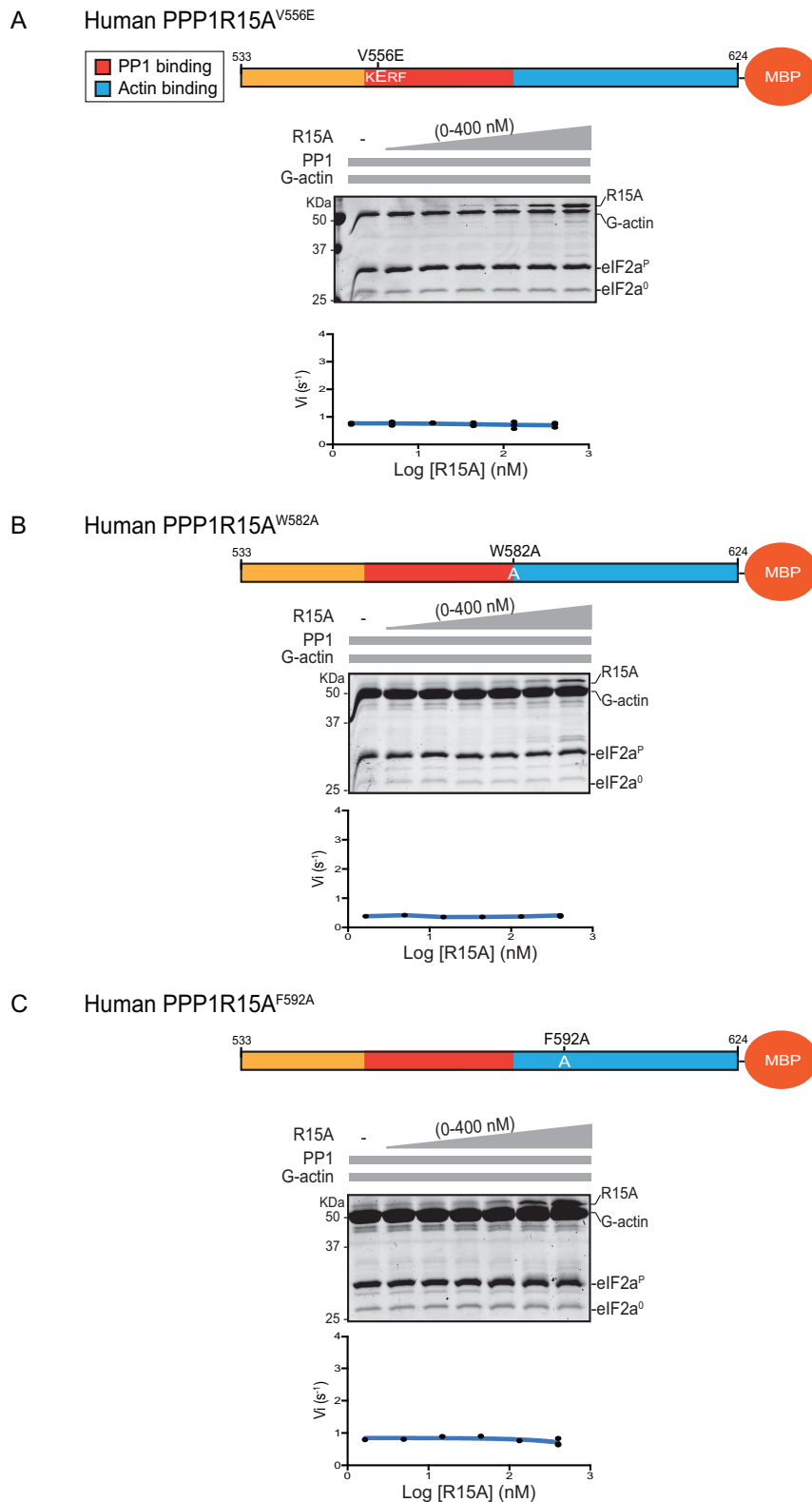


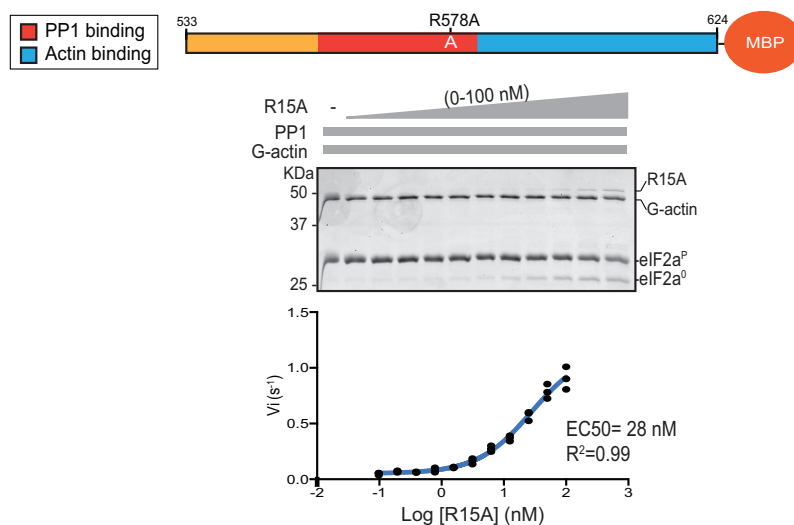
Figure 3. eIF2 α -P dephosphorylation by ternary complexes constituted with human PPP1R15A^{(533-624)V556E}, PPP1R15A^{(533-624)W582A} or PPP1R15A^{(533-624)F592A}. (A) Coomassie-stained PhosTag-SDS-PAGE tracking the dephosphorylation of eIF2 α ^P to eIF2 α ⁰ as in **Figure 2** above, but with PP1[32 nM], G-actin and R15A (0-400 nM). **Figure 3 continued on next page**

Figure 3 continued

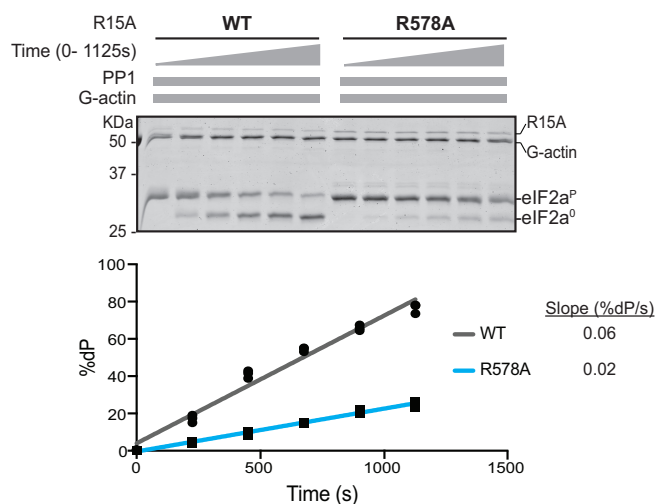
actin [400 nM] and an escalating concentration of mutant human PPP1R15A^{(533-624)V556E}. Shown is a representative of three independent experiments performed. The position of the mutation is provided in the schema above. The plot of initial velocity as a function of PPP1R15A^{(533-624)V556E} derived from three repeats (one shown) is below the SDS-PAGE image. **(B)** As in 'A' above but using human PPP1R15A^{(533-624)W582A} and G-actin [3.7 μM] (Note: only the highest concentration of PPP1R15A was repeated three times). **(C)** As in 'A' above but using human PPP1R15A^{(533-624)F592A} and G-actin [3.7 μM] (Note: only the highest concentration of PPP1R15A was repeated three times).

DOI: [10.7554/eLife.26109.005](https://doi.org/10.7554/eLife.26109.005)

A Human PPP1R15A^{R578A}



B



C

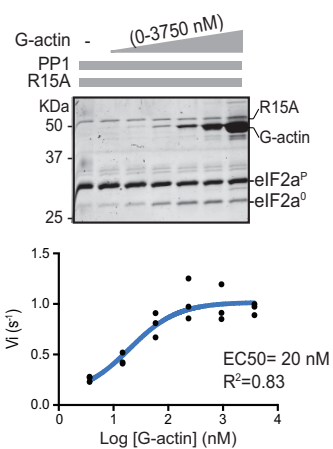


Figure 4. eIF2α-P dephosphorylation by ternary complexes constituted with human PPP1R15A^{(533-624)R578A}. **(A)** Coomassie-stained PhosTag-SDS-PAGE tracking the dephosphorylation of eIF2α^P in a 20 min reaction, as in **Figure 2 and 3** above, but with an escalating concentration of mutant human

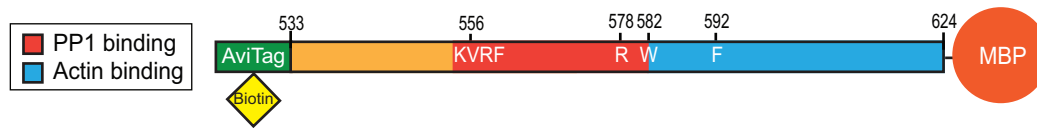
Figure 4 continued on next page

Figure 4 continued

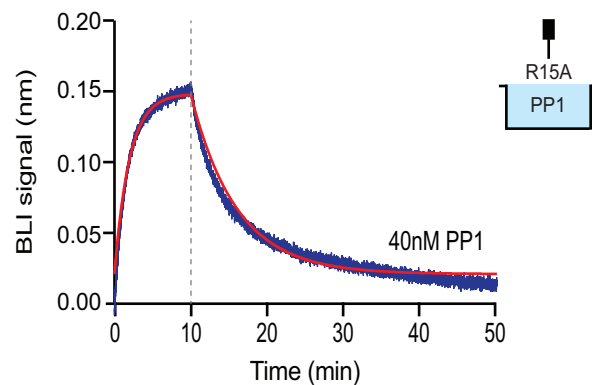
PPP1R15A^{(533-624)R578A}. Shown is a representative of three independent experiments performed. The position of the mutation is provided in the schema above the gel. The plot of initial velocity as a function of PPP1R15A^{(533-624)R578A} derived from three repeats (one shown) is below the SDS-PAGE image. The EC₅₀ for PPP1R15A^{(533-624)R578A} was calculated using the agonist fitting curve in GraphPad Prism V7. (B) Time-course of eIF2 α ^P dephosphorylation using a low concentration of PP1 [0.625 nM], saturating concentrations of G-actin [400 nM], and wildtype [100 nM] or mutant human PPP1R15A^{(533-624)R578A} [100 nM in one assay and 200 nM in the two other assays]. Shown is a representative of three independent experiments performed. Below the gel is a plot of the fraction of substrate dephosphorylated as a function of time derived from three repeats (one shown). The slope of the reaction was derived by fitting the data to a linear model in GraphPad Prism V7. (C) As in 'A' above but with saturating concentration of PPP1R15A^{(533-624)R578A} [100 nM] and escalating concentration of G-actin. Shown is a representative of three independent experiments performed. The plot of initial velocity as a function of G-actin derived from three repeats (one shown) is below the SDS-PAGE image. The EC₅₀ for G-actin was calculated using the agonist fitting curve in GraphPad Prism V7.

DOI: [10.7554/eLife.26109.006](https://doi.org/10.7554/eLife.26109.006)

A Human PPP1R15A

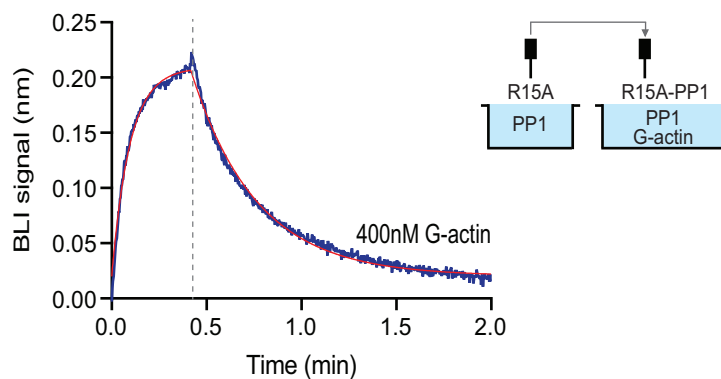


B PP1 association then dissociation



Mean±St Dev	
k_{off} (min ⁻¹)	0.21±0.01
K_d (nM)	20±0.61

C G-actin association then dissociation

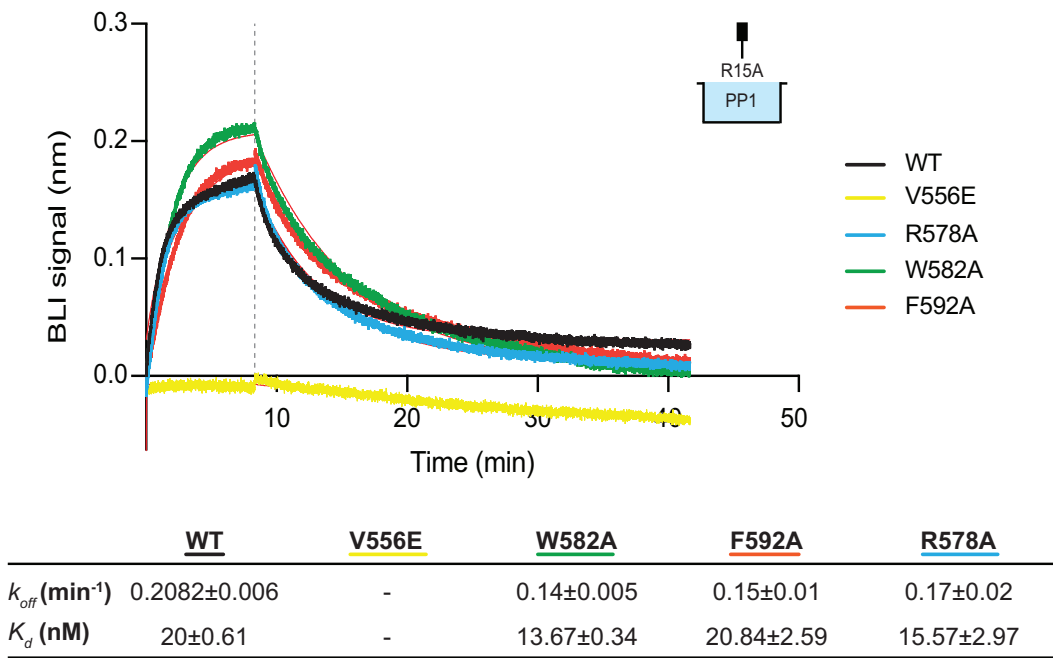


Mean±St Dev	
k_{off} (min ⁻¹)	2.84±0.11
K_d (nM)	151±14.3

Figure 5. Affinity of the components of the tripartite holophosphatase for one another analysed by Bio-Layer Interferometry (BLI). (A) Schema of the biotinylated human PPP1R15A⁵³³⁻⁶²⁴ immobilized onto the BLI biosensor tip. (B) Plot of Bio-Layer Interferometry (BLI) signal as a function of time in a representative experiment (repeated three times) in which immobilized PPP1R15A⁵³³⁻⁶²⁴ was reacted with PP1 [40 nM] in solution (blue trace). The fitting curve using 'association then dissociation' model in GraphPad Prism V7 is shown in red. Vertical dashed line marks the beginning of the dissociation phase. Table summarizes kinetic parameters extracted from fitting curves of three repeats of the experiment shown in left panel (mean ± standard deviation). (C) As in 'B' above, but the immobilized PPP1R15A⁵³³⁻⁶²⁴ was first exposed to PP1 [200 nM], before being exposed to a solution of both PP1 [200 nM] and G-actin [400 nM]. Shown is a representative of an experiment repeated three times.

DOI: [10.7554/eLife.26109.007](https://doi.org/10.7554/eLife.26109.007)

A PP1 association then dissociation



B G-actin association then dissociation

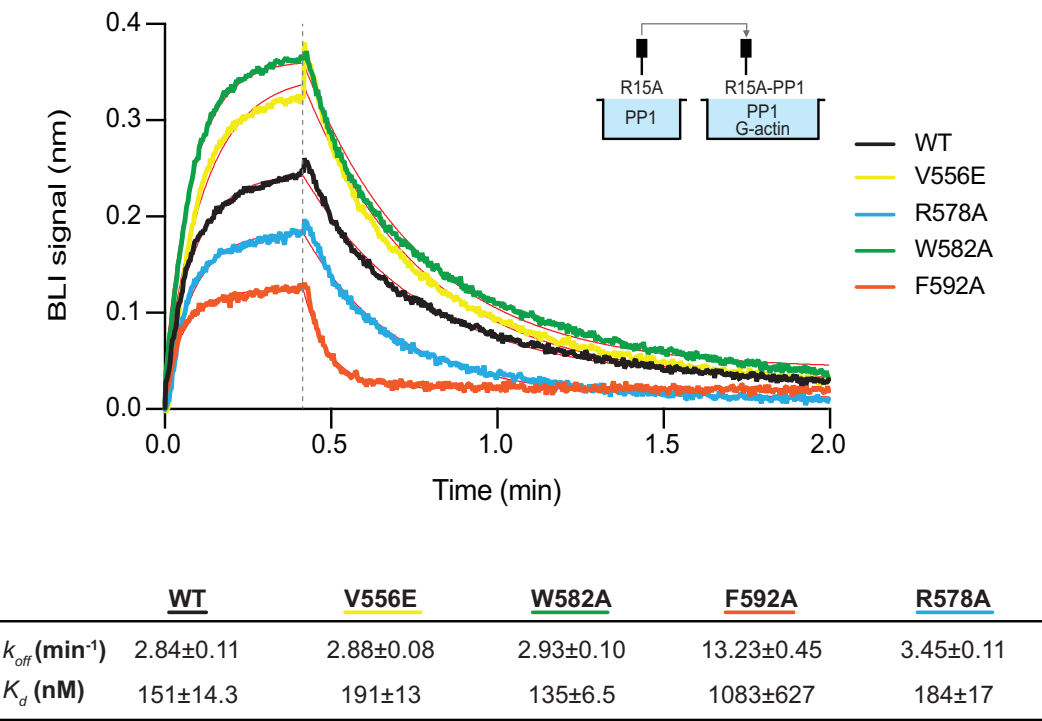


Figure 6. The effect of human PPP1R15A mutations on the affinity of the components of the tripartite holophosphatase for one another analysed by Bio-Layer Interferometry (BLI). (A) Plot of Bio-Layer Interferometry (BLI) signal as a function of time in a representative experiment (repeated three times) Figure 6 continued on next page

Figure 6 continued

in which immobilized wildtype and indicated mutant PPP1R15A⁵³³⁻⁶²⁴ proteins were reacted with PP1 [40 nM] in solution (thick traces). The fitting curve using 'association then dissociation' model in GraphPad Prism V7 is shown in thin red line. Vertical dashed line marks the beginning of the dissociation phase. Table summarizes kinetic parameters extracted from fitting curves of three repeats of the experiment shown in left panel (mean \pm standard deviation). **(B)** As in 'A' above, but the immobilized wildtype and mutant PPP1R15A⁵³³⁻⁶²⁴ probes were first reacted with PP1 [200 nM], before being exposed to a solution of both PP1 [200 nM] and G-actin [400 nM]. Shown is a representative of an experiment repeated three times.

DOI: [10.7554/eLife.26109.008](https://doi.org/10.7554/eLife.26109.008)

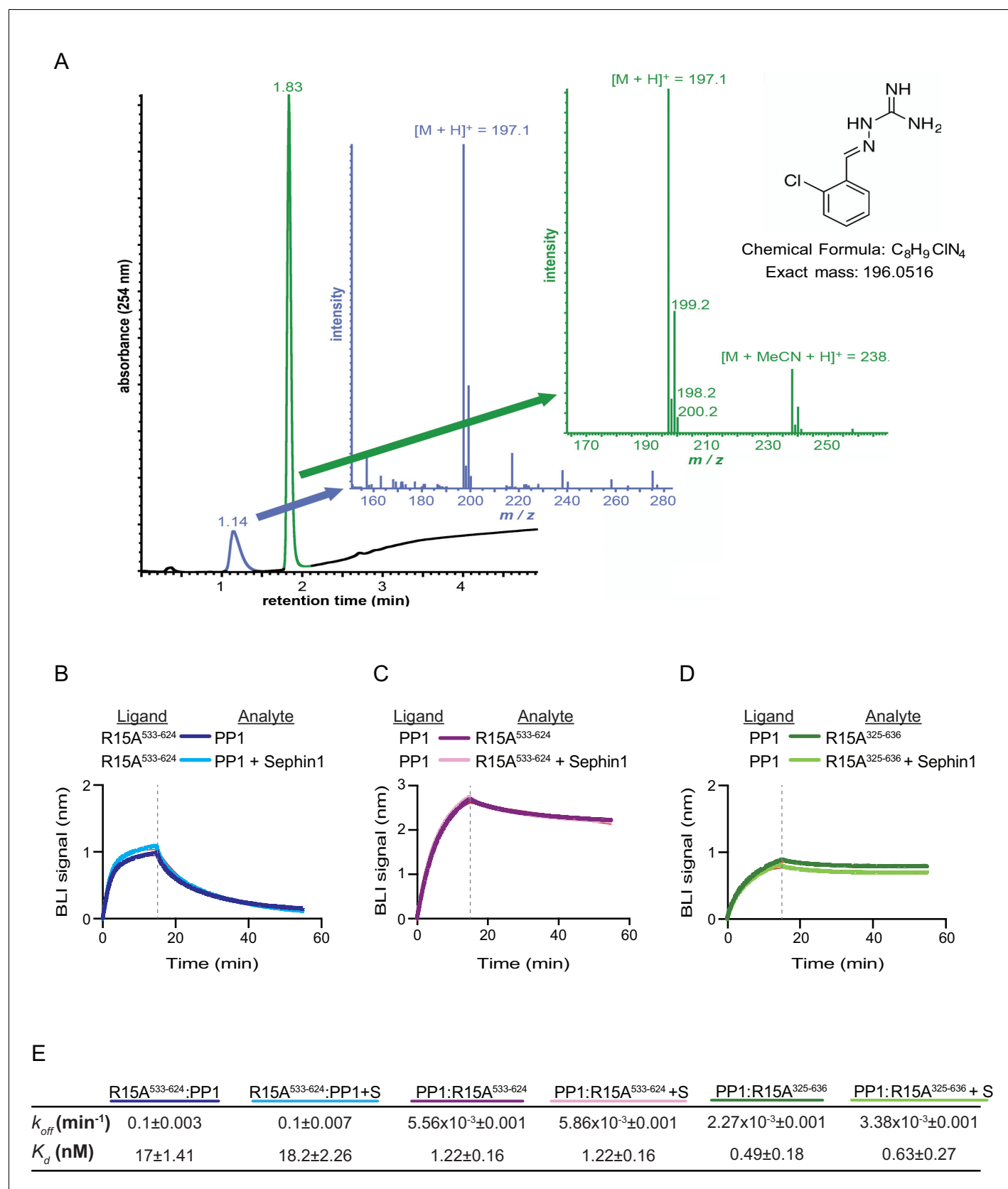


Figure 7. Sephin1's effect on PP1-human PPP1R15A association analysed by Bio-Layer Interferometry (BLI). (A) From left to right: Absorbance trace (at 254 nm) of Sephin1 resolved by reverse-phase HPLC and mass spectra of the minor early (blue) peak eluting at 1.14 min and the major later eluting peak at 1.83 min. Figure 7 continued on next page

Figure 7 continued

(green peak) at 1.83 min. The predicted structure, chemical formula and exact mass of Sephin1, are provided for reference. **(B)** Plot of BLI signal as a function of time of a representative experiment (repeated three times) performed with immobilized PPP1R15A⁵³³⁻⁶²⁴ (Ligand) and PP1 [40 nM] (Analyte). Where indicated, the analyte was mixed with Sephin1 [50 μ M] which was then present during the binding phase of the experiment. **(C)** As in 'B' above but with biotinylated PP1 as the ligand and PPP1R15A⁵³³⁻⁶²⁴ as the analyte, in the absence or presence of Sephin1. **(D)** As in 'B' above but with biotinylated PP1 as the ligand and PPP1R15A³²⁵⁻⁶³⁶ as the analyte, in the absence or presence of Sephin1. **(E)** Table summarizing data extracted from fitting curves of three repeats of the experiments shown above (mean \pm standard deviation).

DOI: [10.7554/eLife.26109.009](https://doi.org/10.7554/eLife.26109.009)

A Human PPP1R15A

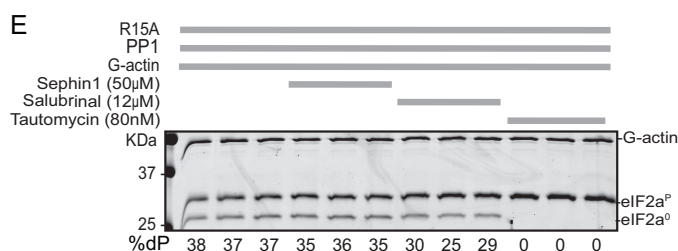
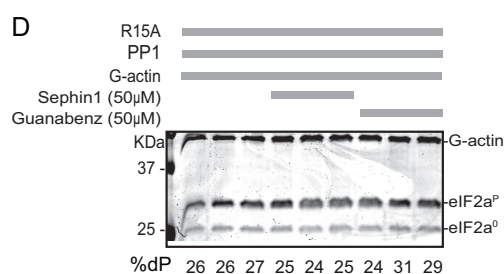
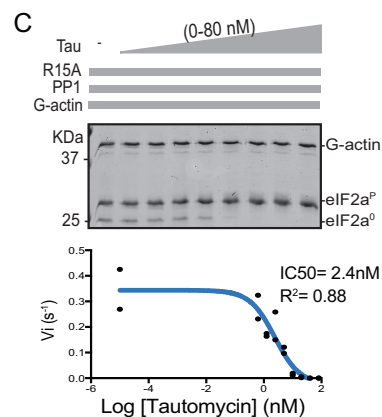
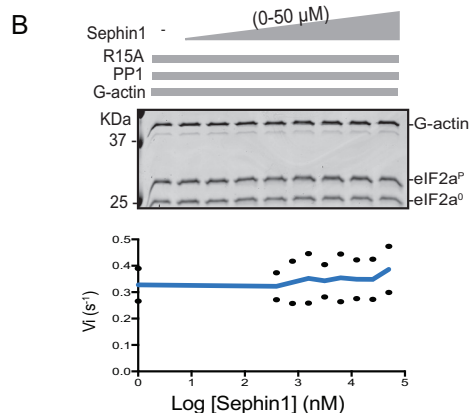
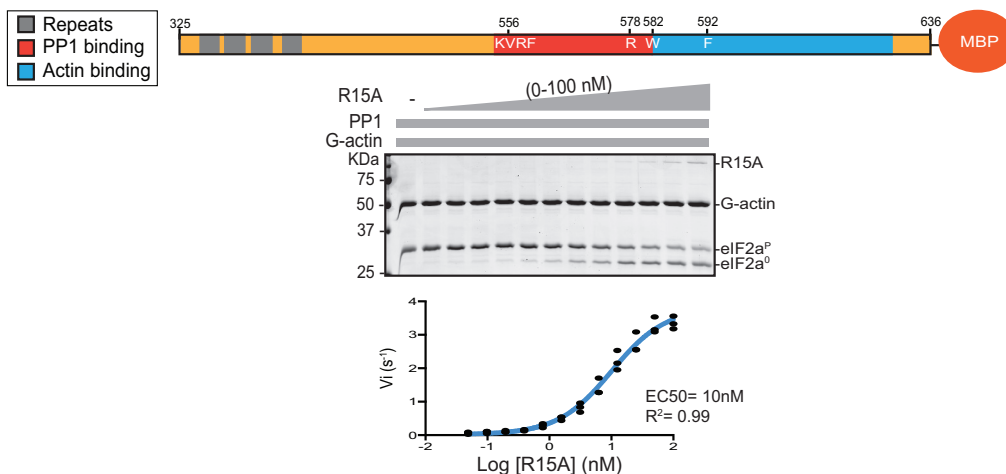


Figure 8. Sephin1's effect on the eIF2α-P dephosphorylation activity of the human PP1-PPP1R15A-G-actin holophosphatase in vitro. (A) Coomassie-stained PhosTag-SDS-PAGE tracking the dephosphorylation of eIF2α^P in 20 min reactions constituted with PP1 [0.625 nM], G-actin [1.5 μM] and an

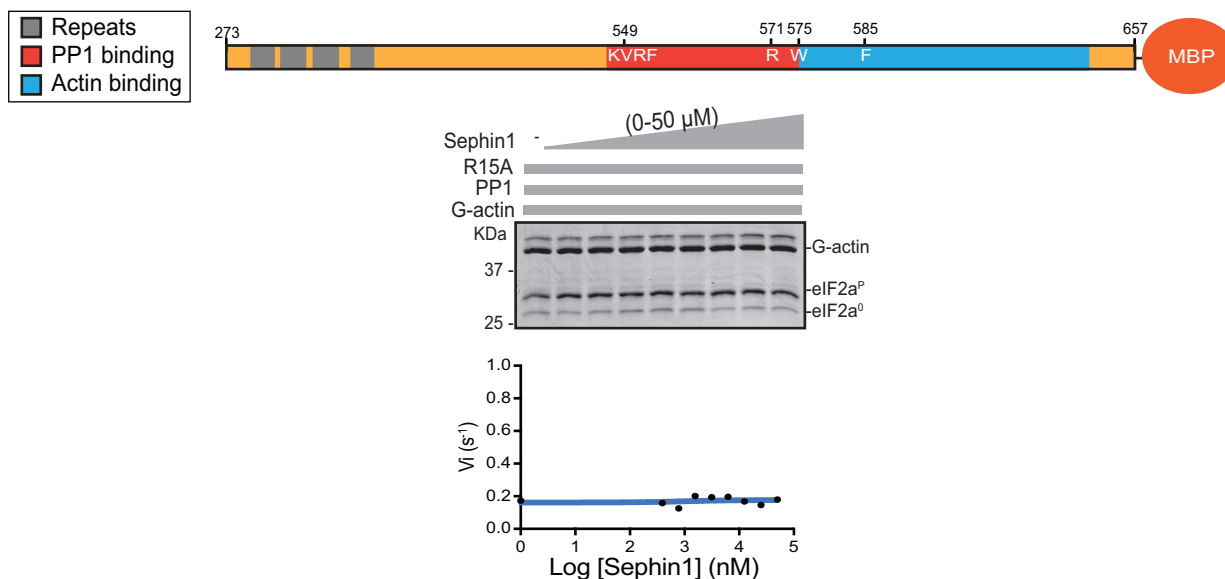
Figure 8 continued on next page

Figure 8 continued

escalating concentration of human PPP1R15A³²⁵⁻⁶³⁶. Shown is a representative of three independent experiments performed. A schema of the human PPP1R15A³²⁵⁻⁶³⁵ construct is shown above the gel. A semi-log₁₀ plot of the initial velocity of eIF2 α ^P dephosphorylation as a function of PPP1R15A³²⁵⁻⁶³⁶ concentration derived from three repeats of the experiment is shown below. The EC₅₀ for PPP1R15A³²⁵⁻⁶³⁶ was calculated using agonist fitting function on GraphPad Prism V7. (B) As in 'A' above, but in the presence of a fixed concentration of PPP1R15A³²⁵⁻⁶³⁶ below the EC₅₀ [2 nM] and escalating concentrations of Sephin1. Shown is a representative of the two independent experiments performed. Plot contains data from the two repeats. (C) As in 'B' above, but in the presence of an escalating concentrations of the PP1 active site inhibitor tautomycin (Tau). Shown is a representative of the two independent experiments performed. Plot contains data from the two repeats. (D) As above, triplicate reactions of eIF2 α -P dephosphorylation conducted in the absence or presence of Sephin1 or the related compound, Guanabenz. (E) As in 'D' using Sephin1, salubrinal or tautomycin. Shown is a representative experiment, (of two repeats).

DOI: [10.7554/eLife.26109.010](https://doi.org/10.7554/eLife.26109.010)

A Mouse PPP1R15A



B

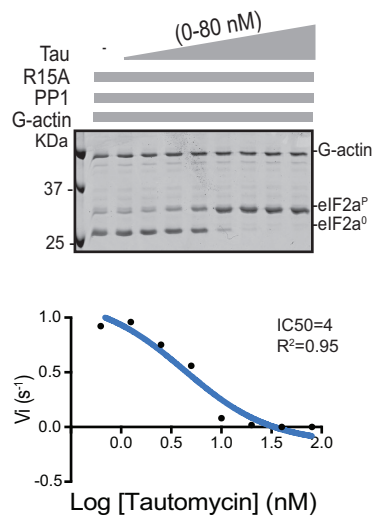


Figure 8—figure supplement 1. Sephin1's effect on the eIF2α-P dephosphorylation activity of the mouse PP1-PPP1R15A-G-actin holophosphatase in vitro. (A) Coomassie-stained PhosTag-SDS-PAGE tracking the dephosphorylation of eIF2α^P in 20 min reactions constituted with mouse PPP1R15A²⁷³⁻⁶⁵⁷ and escalating concentrations of Sephin1. A schema of the mouse PPP1R15A²⁷³⁻⁶⁵⁷ construct is shown above the gel and a semi-log₁₀ plot of the initial velocity as a function of Sephin1 concentration is shown below. (B) As in 'A' above, but in the presence of an escalating concentrations of the PP1 active site inhibitor tautomycin (Tau).

DOI: [10.7554/eLife.26109.011](https://doi.org/10.7554/eLife.26109.011)

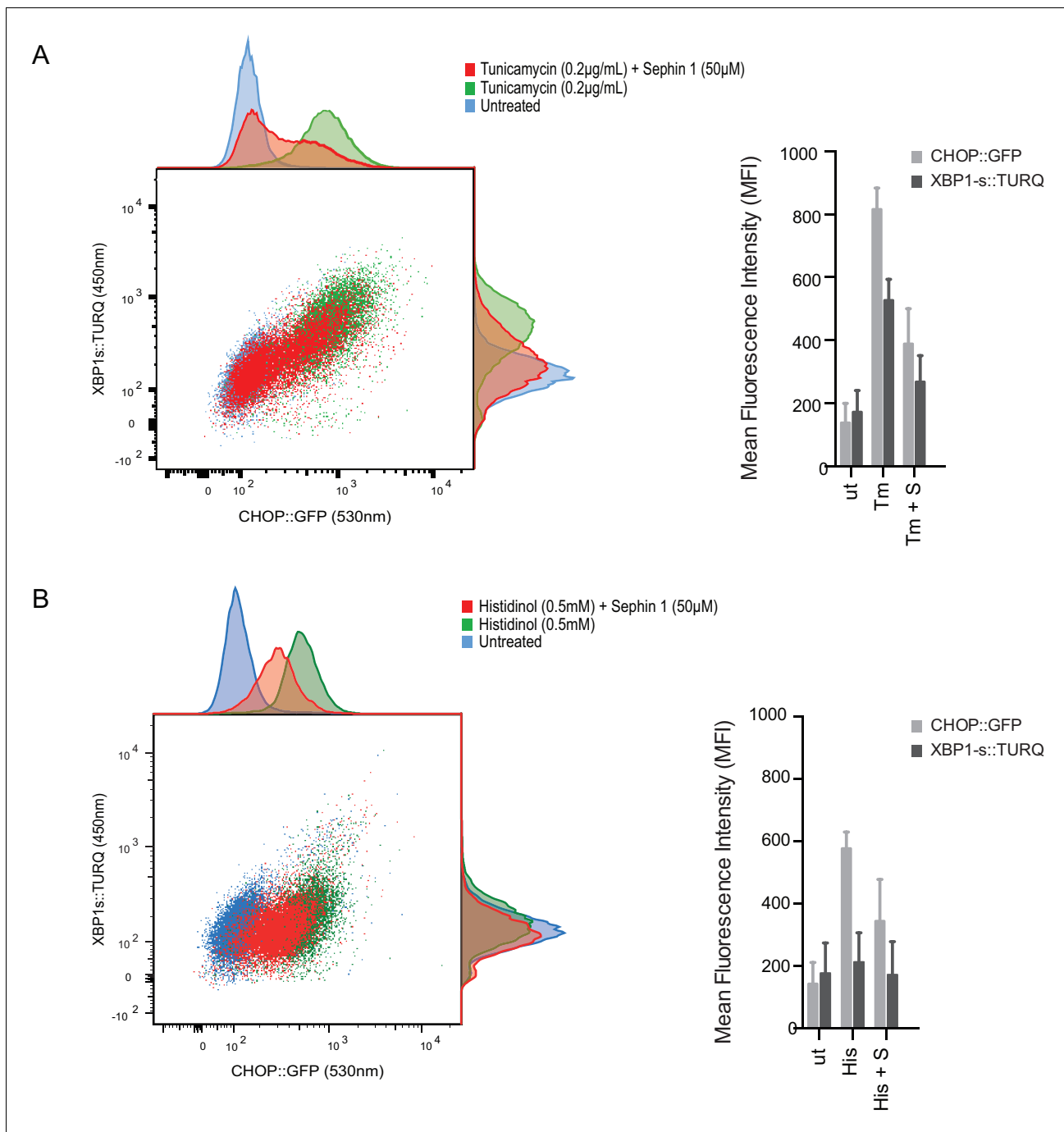


Figure 9. Sephin1 broadly attenuates the ER stress response in cultured CHO cells. (A) Two-dimensional plot of the fluorescence signals derived from CHO cells stably transduced with both a CHOP::GFP reporter (on the horizontal axis, Ex: 488 nm/ Em 530 \pm 30 nm; reflecting mostly ISR activity) and a XBP1::Turquoise reporter (on the vertical axis, Ex: 405 nm/ Em 450 \pm 50 nm; reflecting IRE1 α activity) analysed by flow cytometry. Color-coded signals from untreated cells (blue) or cells exposed to a low concentration of tunicamycin (0.2 $\mu\text{g/mL}$; 20 hr) alone (green) or together with Sephin1 (50 μM , red) are superimposed. Histograms of the distribution of the two reporter signals in the three cell populations are plotted on the corresponding axis and the mean \pm CV (coefficient of variation) of the fluorescence intensity of the two reporters is depicted in the bar diagram to the right. (B) As in 'A' above, but the cells were exposed to histidinol, an ISR inducer that does not promote unfolded protein stress in the ER and does not activate the XBP1::Turquoise reporter. Shown is one of three independent experiments.

DOI: [10.7554/eLife.26109.012](https://doi.org/10.7554/eLife.26109.012)

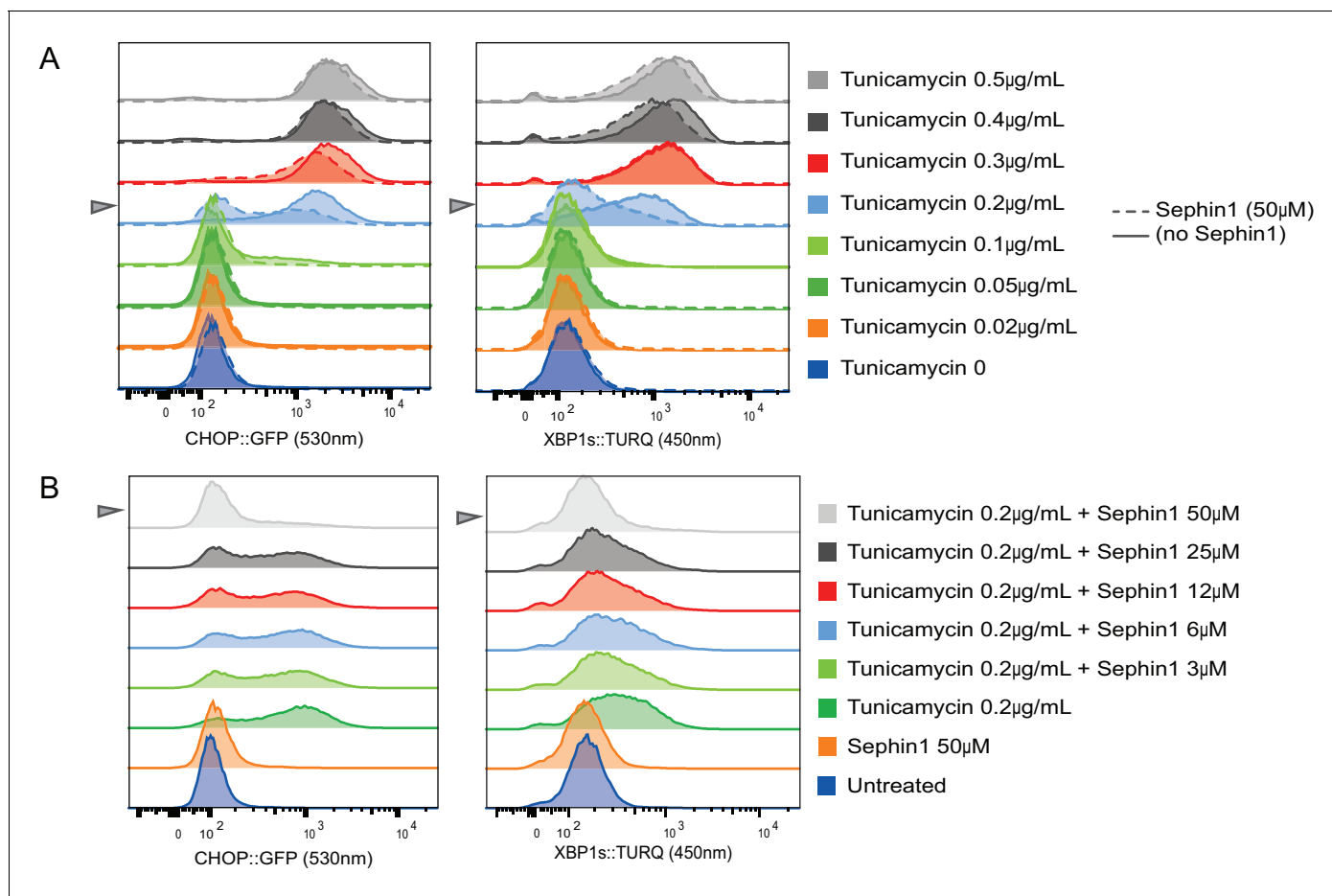


Figure 9—figure supplement 1 . Concentration-dependence of the response of cultured cells to tunicamycin and Sephin1. (A) Histograms of distribution of the fluorescence intensity of the CHOP:GFP reporter (left panel) and XBP1s:turquoise reporter (right panel) in populations of untreated CHO cells and cells exposed for 20 hr to the indicated concentration of tunicamycin in the absence and presence of Sephin1 (50 µM) analysed by flow cytometry. (B) As in 'A' above but the cells were either untreated or exposed to a fixed concentration of tunicamycin (0.2 µg/mL) and varying concentrations of Sephin1.

DOI: [10.7554/eLife.26109.013](https://doi.org/10.7554/eLife.26109.013)

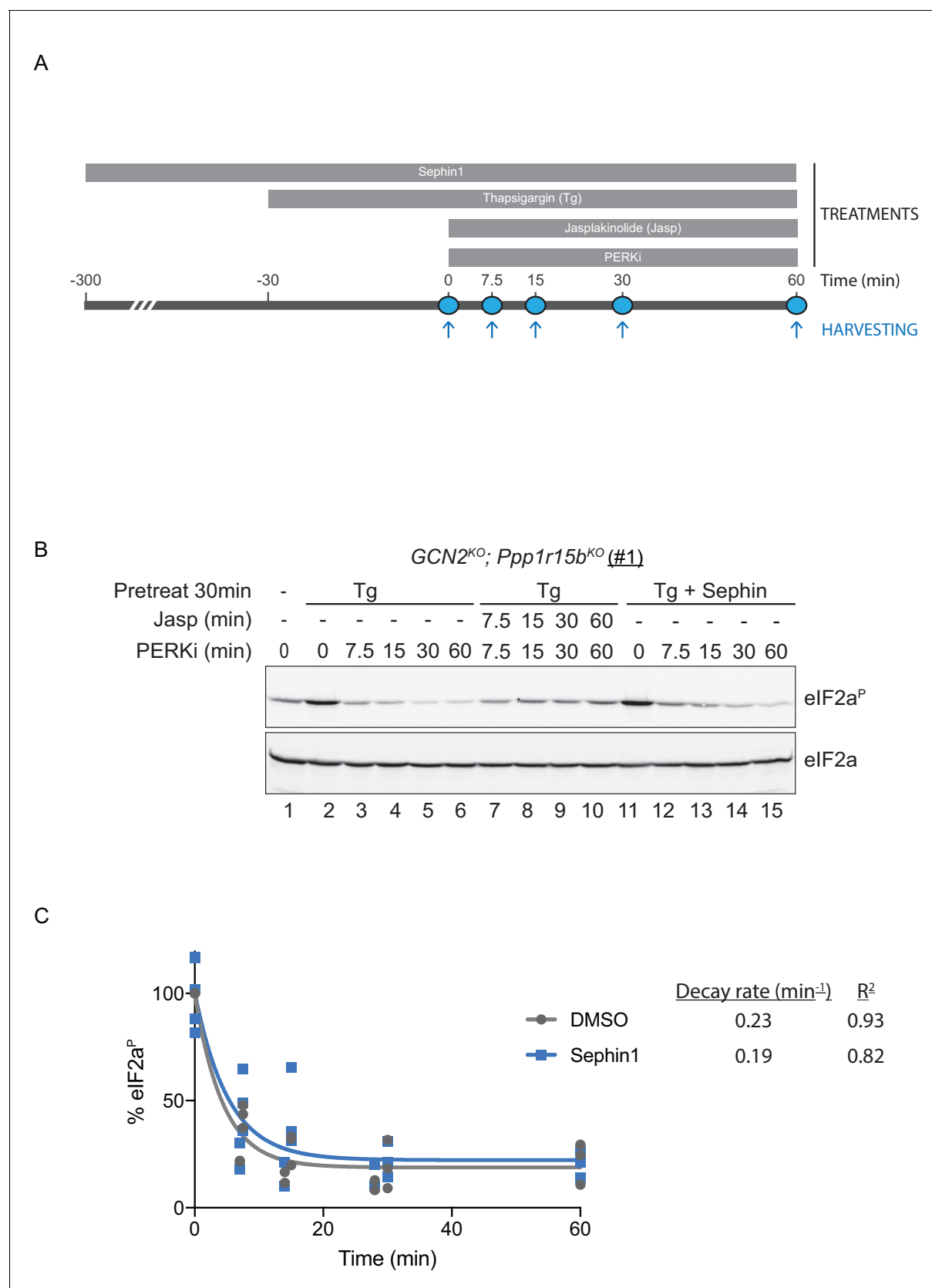


Figure 10. eIF2α^P dephosphorylation in untreated and Sephin1-treated cells. (A) Schema of the kinase shut-off experiment used to evaluate the decay of the eIF2α^P signal in cells. Thapsigargin (300 nM) was added at t = −30 min to the media to activate PERK kinase and induce eIF2α phosphorylation. Figure 10 continued on next page

Figure 10 continued

Sephin1 (50 μ M) was introduced either at $t = -30$ min (alongside thapsigargin, in the experiment shown in panel B below and in **Figure 10—figure supplement 1** panel C) or at $t = -300$ min (**Figure 10—figure supplement 1** panel D). A PERK kinase inhibitor, PERKi/GSK260414A (2 μ M), was added at $t = 0$ to visualize eIF2 α^P dephosphorylation at specified times. (B) Immunoblot of the time-dependent changes in the eIF2 α^P signal of compound-mutant *Ppp1r15b^{KO}; Gcn2^{KO}* CHO-K1 cells (clone #1) treated as in 'A'. Where indicated, the cells were additionally exposed to Sephin1 (50 μ M) or the actin-polymerizing agent Jasplakinolide (1 μ M), which inhibits eIF2 α^P -dephosphorylation by sequestering G-actin. The immunoblot of eIF2 α (lower panel) serves as a loading control. Shown is a representative experiment repeated five times. (C) Plot of the eIF2 α^P signal (normalised to the value at $t = 0$ of the vehicle only (DMSO) sample) as a function of time derived from five independent experiments. The data have been fitted to an exponential decay curve (grey solid line for the vehicle and blue solid line for the Sephin1-treated sample). The exponential decay rate and the R^2 of the fit are indicated.

DOI: [10.7554/eLife.26109.014](https://doi.org/10.7554/eLife.26109.014)

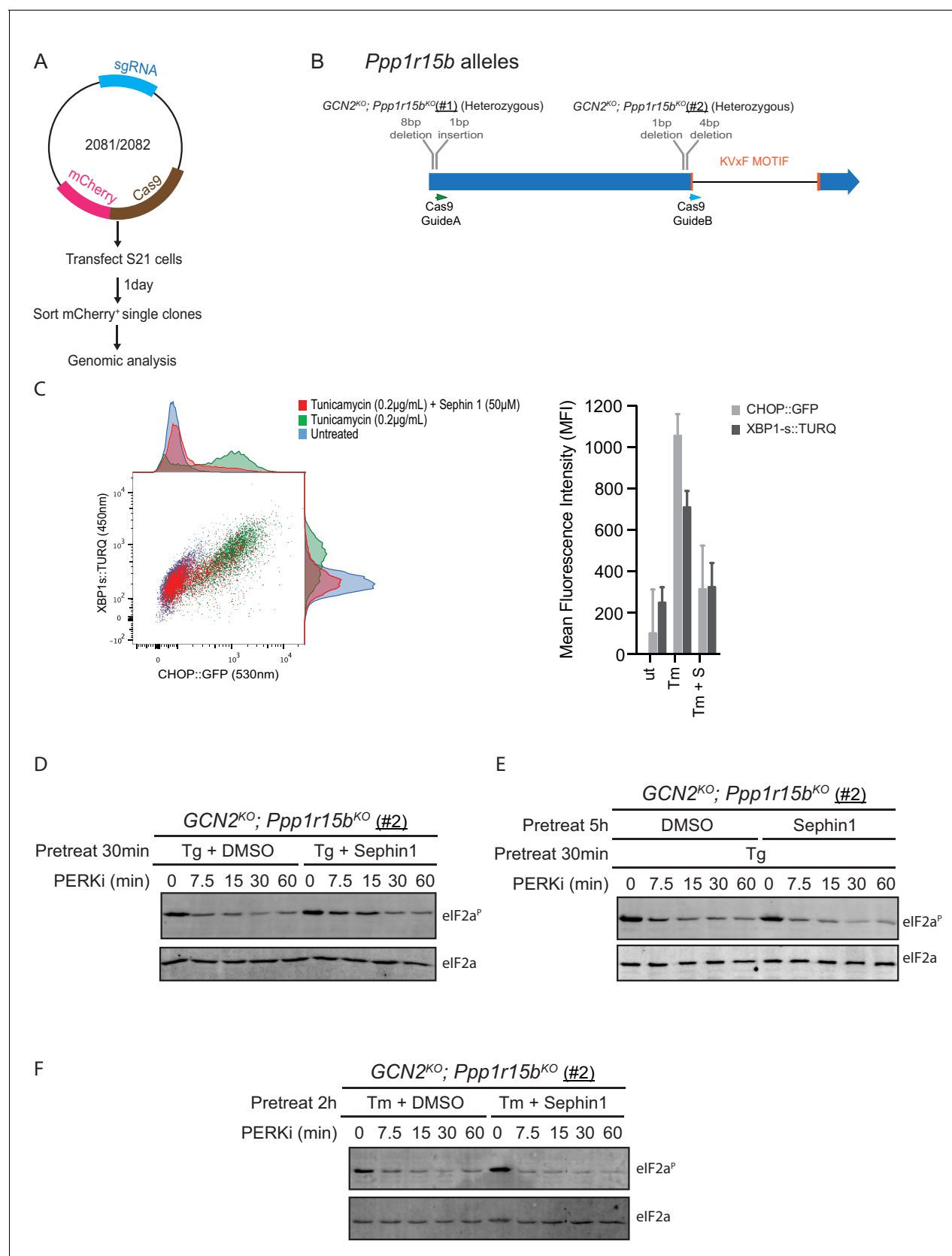


Figure 10—figure supplement 1. Analysis of Sephin1 in a different *Ppp1r15b* mutant cell line. (A) Schema of the procedure to create dual reporter (CHOP::GFP, XBP1s::Turquoise) compound mutant *Gcn2*^{KO}; *Ppp1r15b*^{KO} CHO-K1 cells using the CRISPR-Cas9 system. (B) Schema of the mutant alleles. Figure 10—figure supplement 1 continued on next page

Figure 10—figure supplement 1 continued

The two coding exons of wildtype hamster *Ppp1r15b* are denoted as is the region encoding the PP1-binding RVxF motif (KVTF, in PPP1R15B) and the positions of the guide RNAs used to direct the Cas9-mediated double strand breaks. (C) Two-dimensional plot and histograms of the fluorescent signal of the CHOP::GFP and XBP1s::Turquoise reporters in compound *Ppp1r15b*^{KO}; *Gcn2*^{KO} CHO-K1 cells (clone #2). Where indicated, the cells were exposed to a low concentration of tunicamycin (0.2 µg/mL; 20 hr) alone or together with Sephin1 (50 µM). The mean ± CV (coefficient of variation) of the fluorescence intensity of the two reporters is displayed in the bar diagram. Shown is one of three independent experiments. (D) As in 'Figure 10B' but using *Ppp1r15b*^{KO}; *Gcn2*^{KO} (clone #2). (E) As in 'D' above, but Sephin1 pretreatment was extended to 5 hr, before the kinase shut-off procedure, and continued throughout. (F) As in 'D' above, but substituting tunicamycin (2.5 µg/mL; 2 hr) for thapsigargin as the PERK inducer. Shown is a representative experiment (of two repeats).

DOI: [10.7554/eLife.26109.015](https://doi.org/10.7554/eLife.26109.015)

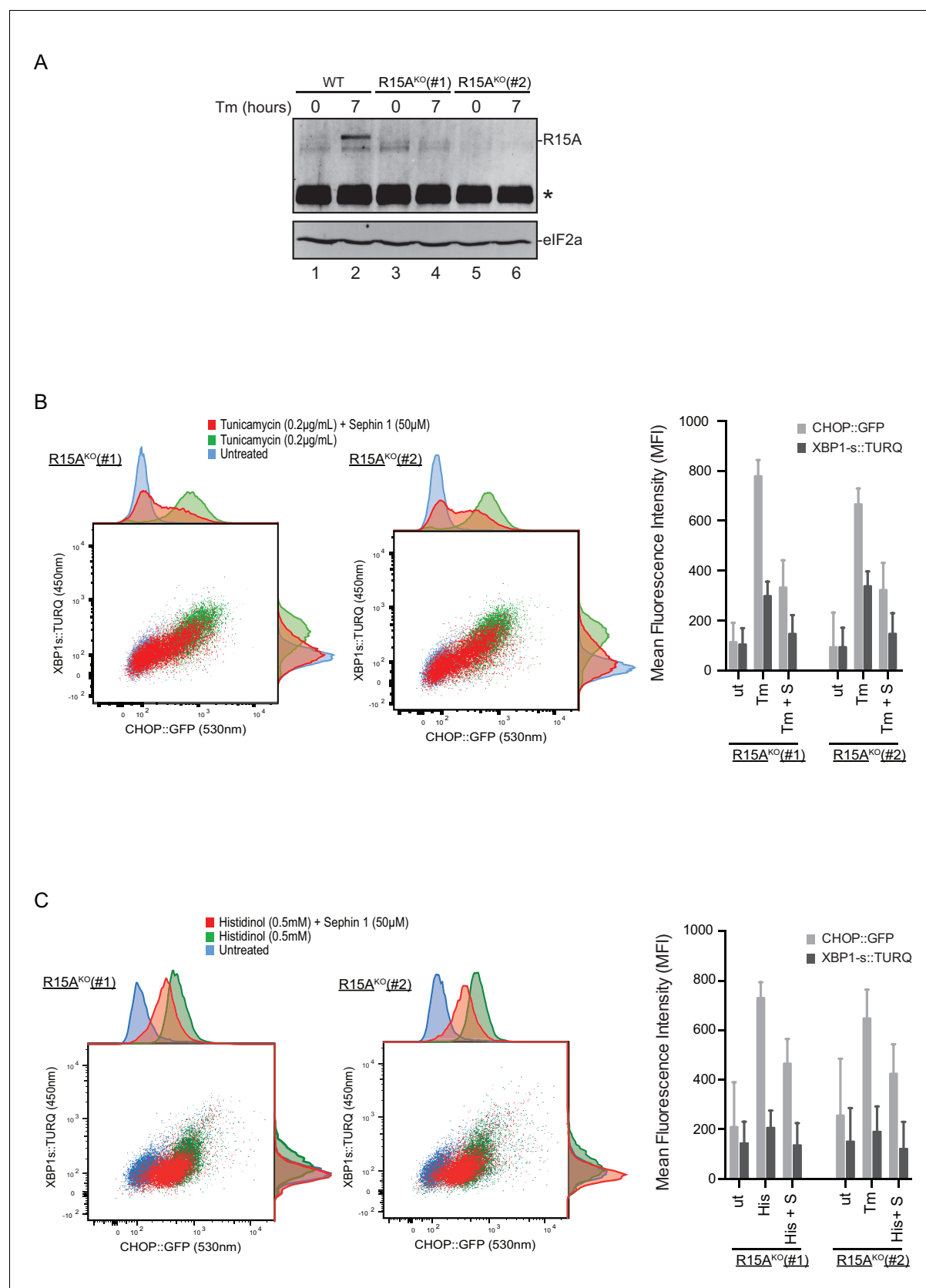


Figure 11. Cells lacking PPP1R15A remain responsive to Sephin1. (A) Immunoblot of endogenous PPP1R15A recovered by immunoprecipitation (using an anti-PPP1R15A antibody conjugated to Protein A Sepharose) from untreated and tunicamycin exposed parental cells and cells from two different

Figure 11 continued on next page

Figure 11 continued

Ppp1r15a^{KO} CHO-K1 clones. The position of PPP1R15A is indicated and the immunoglobulin heavy-chain is marked with an asterisks. The immunoblot of eIF2 α (lower panel) serves as a loading control for the content of cellular protein in the lysates. (B) Two-dimensional plot and histograms of the fluorescent signal of the CHOP::GFP and XBP1s::Turquoise reporters in the two *Ppp1r15a*^{KO} CHO-K1 clones. Where indicated, the cells were exposed to a low concentration of tunicamycin (0.2 μ g/mL; 20 hr) alone or together with Sephin1 (50 μ M). The mean \pm CV (coefficient of variation) of the fluorescence intensity of the two reporters in each of the two clones is displayed in the bar diagram. Shown is one of three independent experiments. (C) As in 'C' above, but cells were exposed to histidinol. Shown is one of three independent experiments.

DOI: [10.7554/eLife.26109.016](https://doi.org/10.7554/eLife.26109.016)

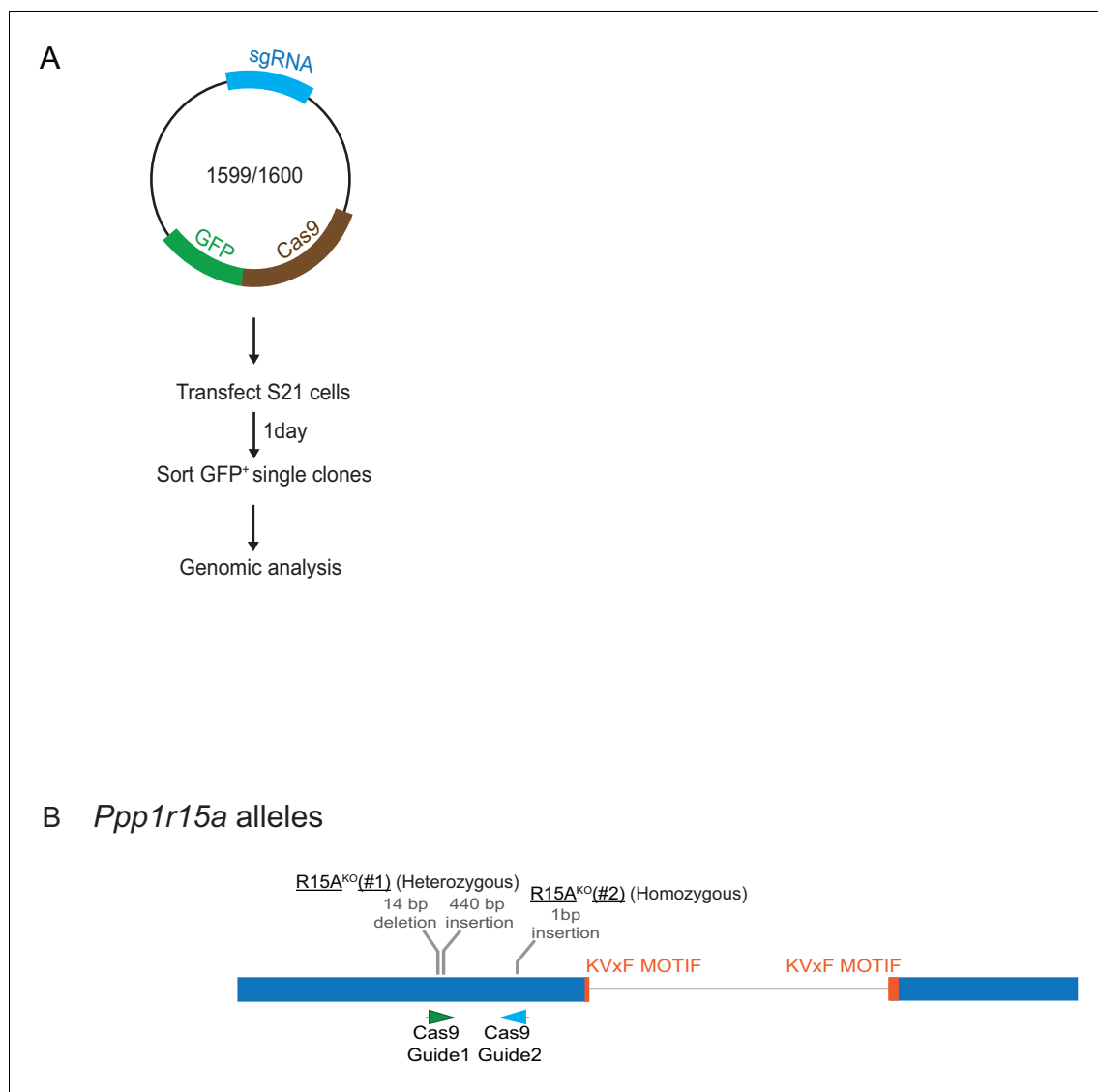


Figure 11—figure supplement 1 . Mutant *Ppp1r15a* alleles. (A) Schema of the procedure to create dual reporter (CHOP::GFP, XBP1s::Turquoise) *Ppp1r15a*^{KO} CHO-K1 cells using the CRISPR-Cas9 system. (B) Schema of the mutant alleles. The two coding exons of wildtype hamster *Ppp1r15a* are denoted as is the region encoding the crucial RVxF motif (KVHF, in PPP1R15A) and the positions of the guide RNAs used to direct the Cas9-mediated double strand breaks.

DOI: [10.7554/eLife.26109.017](https://doi.org/10.7554/eLife.26109.017)

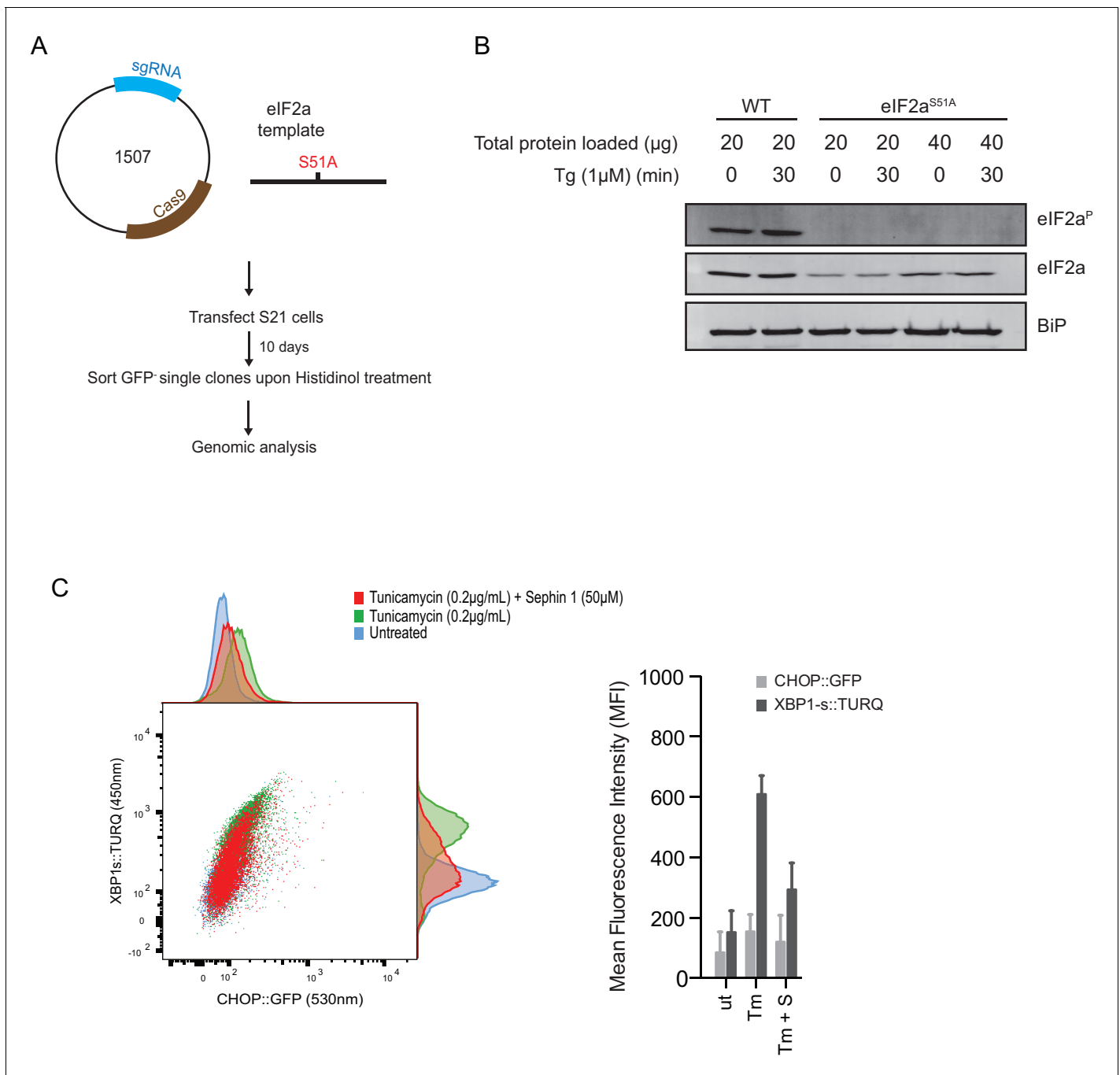


Figure 12. ISR-deficient *Eif2s1^{S51A}* (eIF2α^{S51A}) cells retain their responsiveness to Sephin1. (A) Schematic representation of procedure used to create dual reporter (CHOP::GFP, XBP1s::Turquoise) *Eif2s1^{S51A}* (eIF2α^{S51A}) CHO-K1 cells using CRISPR-Cas9 system. (B) Immunoblot of CHO-K1 cell lysates using anti-eIF2α^P (upper panel), anti-eIF2α (middle panel) and anti-BiP (lower panel) antibodies. Two-fold more cell lysate was loaded onto lanes 5 and 6 to compensate for the lower eIF2α content of the haploid mutant *Eif2s1^{S51A}* cells. (C) Two-dimensional plot and histograms of the fluorescent signal of the CHOP::GFP and XBP1s::Turquoise reporters in the *Eif2s1^{S51A}* CHO-K1 cells. Where indicated, the cells were exposed to a low concentration of tunicamycin (0.2 μg/mL; 20 hr) alone or together with Sephin1 (50 μM). The mean ± CV (coefficient of variation) of the fluorescence intensity of the two reporters in each of the two clones is displayed in the bar diagram. Shown is representative experiment of two independent experiments performed. Note the blunted expression of CHOP::GFP wrought by the ISR-defect imposed by the *Eif2s1^{S51A}* mutation.

DOI: 10.7554/eLife.26109.018